INTERNATIONAL PROGRAMS AND ACTIVITIES RELATED TO DEGRADATION OF CANDIDATE WASTE PACKAGE MATERIALS FOR GEOLOGICAL DISPOSAL OF SPENT NUCLEAR FUEL AND HIGH-LEVEL WASTE

Prepared for

U.S. Nuclear Regulatory Commission
Contract NRC–HQ–12–C–02–0089

Prepared by

Xihua He[1]
Tae Ahn[2]

[1]Center for Nuclear Waste Regulatory Analyses
San Antonio, Texas

[2]U.S. Nuclear Regulatory Commission
Washington, DC

February 2020

ABSTRACT

Several countries have been exploring the feasibility of spent nuclear fuel and high-level radioactive waste disposal in deep geological repositories. Copper (Cu), carbon steel, and titanium (Ti) alloys are three of the candidate metallic materials for waste containment in repositories in clay, crystalline, sedimentary, or salt rocks. Stainless steels are mostly under consideration as canister materials for low- and intermediate-level waste isolation, for which absolute containment is not critical and a lifetime in thousands of years is not required. The in-house performance assessment model, Scoping of Options and Analyzing Risk (SOAR), developed by the U.S. Nuclear Regulatory Commission (NRC) and the Center for Nuclear Waste Regulatory Analyses (CNWRA®), incorporates key information related to degradation of metallic canisters from the literature up to 2011. Over the years, NRC-sponsored studies on corrosion of Cu, carbon steel, and Ti under repository-relevant environments have been summarized in a series of reports and papers. The objective of the current work was to analyze and compare Cu, carbon steel, and Ti corrosion rates and degradation mechanisms under various radioactive waste disposal environments associated with different repository designs. The analyses and comparisons were based on laboratory data from NRC-sponsored studies and literature data, mostly after 2011. Selected literature data on stainless steel also were included for completeness.

Led by Sweden and Canada, significant research took place over the past 20 years to determine Cu corrosion rates and hydrogen (H_2) generation in anoxic pure water. The literature shows that under anoxic conditions, corrosion rates can be enhanced by hydrogen sulfide and chloride. Researchers from Swedish Nuclear Fuel and Waste Management Co. (SKB) in Sweden argued that H_2 observed from tests in anoxic water is not produced from Cu corrosion. Instead, the SKB researchers argued, H_2 pre-exists as dissolved hydrogen at interstitial and trap sites in the Cu specimens or from the test cell. In an updated SKB analysis published in 2019 to address issues raised by an environmental court, SKB concluded that specific Cu corrosion issues were of minor consequence to individual dose estimates because (i) corrosion in anoxic water accompanied by H_2 generation is unlikely and (ii) availability of hydrogen sulfide to enhance corrosion is limited in the repository. Considering the effects of chloride and other species and the variability of environmental conditions, it is recommended to re-examine the SOAR model for Cu corrosion in anoxic conditions to account for the effects of both sulfide and chloride.

Carbon steel corrodes actively in clay porewaters, with corrosion rates depending on the properties of the clay, chemical composition of porewater, temperature, radiation level, material properties, and test duration. Most studies report that (i) the carbon steel corrosion rate decreases with time in both oxic and anoxic conditions, (ii) magnetite is the predominant corrosion product in anoxic conditions, (iii) the corrosion product can be protective, and (iv) corrosion products can interact with the clay and change its properties. In anoxic alkaline conditions over pH 10 to 13, effects of chloride, sulfide, and thiosulfate on passivity of the carbon steel and the localized corrosion resistance are not unequivocally established (different experimental programs suggest different conclusions). Bacterial activity can enhance corrosion significantly; however, long-term effects on waste container performance remain uncertain. Stress corrosion cracking (SCC) and hydrogen embrittlement resistance are not consistently reported, depending on types of material, thermal, environmental, and mechanical conditions, and test duration. The potential risk of SCC needs to be evaluated further for long-term analyses of repository performance because SCC can be a more detrimental degradation mode than general corrosion and localized corrosion. Incorporation of SCC in the SOAR canister failure model should be reconsidered after gathering more information.

The corrosion performance of different grades of Ti can vary significantly. In addition to general corrosion, hydrogen embrittlement can be an important degradation mode for Ti and should be evaluated for incorporation into SOAR. In oxic conditions, stainless steel can be susceptible to pitting corrosion and SCC, which could limit the lifetime of stainless steel material in repository settings. Based on literature information, SCC is another degradation mechanism for stainless steel to be considered for incorporation in SOAR, especially under oxic conditions.

CONTENTS

LIST OF FIGURES

Figure Page

LIST OF TABLES

ABBREVIATION/ACRONYMS

CNWRA®	Center for Nuclear Waste Regulatory Analyses
Cu	copper
EIS	electrochemical impedance spectroscopy
EPRI	Electric Power Research Institute
HLW	high lever radioactive waste
IN	Information Notice
MIC	microbiologically influenced corrosion
NRC	U.S. Nuclear Regulatory Commission
OCP	open-circuit potential
SCC	stress corrosion cracking
SKB	Swedish Nuclear Fuel and Waste Management Co.
SNF	spent nuclear fuel
SOAR	Scoping of Options and Analyzing Risk
Ti	titanium

ACKNOWLEDGMENTS

This report was prepared to document work performed by the Center for Nuclear Waste Regulatory Analyses (CNWRA®) for the U.S. Nuclear Regulatory Commission (NRC) under Contract No. 31310018D0001. The activities reported here were performed on behalf of the NRC Office of Nuclear Material Safety and Safeguards, Division of Fuel Management. The report is an independent product of CNWRA and does not necessarily reflect the views or regulatory position of NRC. The NRC staff views expressed herein are preliminary and do not constitute a final judgment or determination of the matters addressed or of the acceptability of any licensing action that may be under consideration at NRC.

The authors acknowledge the valuable contributions of the NRC Project Manager, J. Gwo, for guidance, feedback, and information provided over the duration of this project.

The authors thank O. Pensado for technical review and D. Pickett for programmatic review. The authors also thank A. Ramos for support in report preparation.

QUALITY OF DATA, ANALYSES, AND CODE DEVELOPMENT

DATA: There are no original CNWRA-generated data in this report. Sources of other data should be consulted for determining the level of quality of those data.

ANALYSES AND CODES: No software subject to control under Technical Operating Procedure TOP-018 was used in this study.

1 INTRODUCTION

Several countries have been exploring the feasibility of spent nuclear fuel (SNF) and high-level radioactive waste (HLW) disposal in deep geological repositories, including Belgium, Canada, China, Czech Republic, Finland, France, Germany, Japan, Korea, Sweden, and Switzerland (King, 2017, 2013a). Copper (Cu), carbon steel, and titanium (Ti) alloys are three candidate metallic materials for canisters for radioactive waste containment in a geologic repository in clay, crystalline, sedimentary, or salt rocks. Among the three materials, carbon steel and Cu are considered the most likely candidates, with extensive research performed worldwide over the years. Various national SNF and HLW disposal programs, as well as international collaborative projects, have accumulated a large amount of technical data related to waste package material degradation. The in-house performance assessment model, Scoping of Options and Analyzing Risk (SOAR) developed by the U.S. Nuclear Regulatory Commission (NRC) and the Center for Nuclear Waste Regulatory Analyses (CNWRA®) incorporates key information related to degradation of metallic canisters from the literature up to 2011. Data to define corrosion rates of waste container materials in SOAR was described in detail in papers by He et al. (2011) and Jung et al. (2011). The corrosion model implemented in SOAR is described in its most recent user guide (NRC and CNWRA, 2019).

Over the years, NRC-sponsored studies on corrosion of Cu, carbon steel, and Ti under repository-relevant environments have been summarized in a series of reports (He and Ahn, 2019a, 2018, 2017a, 2017b; He et al., 2015) and papers (He and Ahn, 2019b; He et al., 2018, 2017). The objective of the current work was to analyze and compare Cu, carbon steel, and Ti corrosion rates and degradation mechanisms under various radioactive waste disposal environments associated with different repository designs. The analyses and comparison were based on laboratory data from NRC-sponsored studies and literature data, mostly after 2011. In contrast with Cu, carbon steel, and Ti alloys, stainless steels are mostly under consideration as canister materials for low- and intermediate-level waste isolation, for which absolute containment is not critical and lifetime in thousands of years is not required. Because the SOAR model includes stainless steel as canister material, this work also updates literature data on stainless steel for completeness. The following information was obtained from the analysis:

(i). Environmental variables affecting waste package material corrosion, including the effects of the fate and transport of chemical species in the near field of a repository

(ii). Controlling mechanisms (e.g., electrochemical versus chemical dissolution) affecting waste package material degradation

(iii). Uncertainty of measured and theoretical corrosion rates with respect to repository environmental variables

The detailed information from the literature and NRC-sponsored studies is presented in Chapter 2 and is summarized in Chapter 3 in tables to facilitate potential incorporation into SOAR.

2 DEGRADATION OF COPPER, CARBON STEEL, TITANIUM, AND STAINLESS STEEL AS CANDIDATE WASTE PACKAGE MATERIALS

Degradation of waste package materials depends on thermal, environmental, radiological, and mechanical conditions. In the scientific literature, the evolution of the environmental conditions in a deep geologic repository is commonly divided into three periods:

Period I—Oxidizing period: This is the initial period after repository closure during which some O_2 is trapped in the environment, temperature is elevated by the decay heat from the nuclear waste, and the radiation level is relatively high. Temperature gradients would move water away from the waste container surface. According to King and Kolár (2019), the trapped O_2 amount is about 1 mol/m^2 to 10 mol/m^2 for the different repository designs in various countries. If corrosion proceeds in the form of general corrosion driven by the trapped oxygen, the corrosion depth is in the order of a few tens to a few hundreds of micrometers. Compared with container wall thicknesses in the range of several millimeters to several centimeters, the general corrosion depth associated with the initially trapped oxygen is negligible. If the O_2 distribution was nonuniform or if there was nonuniform distribution of deliquescent salt deposits on the container surface, localized corrosion might arise leading to larger penetration depth, which might be a concern for the waste container. This initial oxidizing period could last tens to hundreds of years, depending on the repository design. Recent studies from a full-scale in situ test suggest that it may last only several weeks or months because O_2 is consumed by reaction with oxidizable minerals and aerobic bacteria (Necib et al., 2017a).

Period II—Transient reducing period: This is the time following Period I after all of the O_2 is consumed. The environment becomes anoxic while the repository is still unsaturated. Corrosion during this period could be supported by the cathodic reduction of H_2O or other chemical species such as HS^-. Corrosion could be general or localized depending on the distribution of moisture, the chemical composition of solution, and surface deposits. As the water starts moving toward the container, the surface wetness may be nonuniform, which could lead to separation of anodic and cathodic sites.

Period III—Stable reducing period: This is the predominant period during which the repository is saturated and anoxic. If the host rock has low permeability, saturation may take tens of thousands of years. According to SKB (2019), the saturation time of the bentonite buffer is expected to vary between a few tens to a few thousand years, depending on the position of deposition holes with respect to water conducting fractures in the KBS-3 repository. As was the case for Period II, the corrosion process could be supported by the cathodic reduction of H_2O or other chemical species such as HS^-.

The following sections discuss and summarize literature information on four candidate waste package materials: (i) Cu, (ii) carbon steel, (iii) Ti alloys, and (iv) stainless steel.

2.1 Copper Corrosion

Cu has been proposed as a waste package material or an alternative material in a number of HLW repository programs, including those in Canada, Finland, Japan, Korea, Switzerland, and Sweden. The repository would be located several hundred meters below the water table in stable host rock with deposition holes and tunnels containing bentonite-based backfill and buffer structures. In the past 20 to 30 years, there has been considerable work on the corrosion of Cu

in clay systems. Actively investigated areas include (i) general corrosion and pitting corrosion in the early oxidizing period; (ii) corrosion in anoxic pure water; (iii) general corrosion, pitting corrosion, stress corrosion cracking (SCC), and hydrogen embrittlement in anoxic environments that include HS^-; and (iv) corrosion of thin Cu coatings formed by cold spray or electrodeposition compared to wrought Cu.

2.1.1 Cu corrosion in the oxidizing period

According to the Pourbaix thermodynamic stability diagram, in the presence of an oxidant, typically O_2, corrosion of Cu is likely to occur because the H_2O/O_2 equilibrium potential is above the Cu/Cu^+, Cu^+/Cu^{2+}, or Cu/Cu^{2+} equilibrium potentials (Pourbaix, 1974). In this case, O_2 functions as an acceptor for the electrons produced by Cu oxidation. Cu corrosion behavior in oxic conditions has been well studied and a large database is available in the literature. Corrosion rates vary depending on the O_2 concentration in solution, and are predominantly in the range of several hundredths of a micrometer per year to several micrometers per year (Jung et al., 2011). During the early oxidizing period, γ radiation might produce nitric acid (HNO_3), oxidants such as hydrogen peroxide, and H_2, depending on the radiation level. HNO_3 and oxidants can enhance Cu corrosion. Lousada et al. (2016) reports that γ radiation at a total dose of 69 kGy enhanced hydrogen absorption in Cu significantly compared to absorption into unirradiated Cu, and the amount of hydrogen absorbed depends on the accumulated radiation dose to the Cu metal. Ibrahim et al. (2018) observed that corrosion of Cu occurring under exposure to aerated vapor yielded initially a film of cuprous oxide (Cu_2O), and eventually cupric oxide (CuO). Based on limited studies, these authors were uncertain if this corrosion was accelerated by γ-radiation at a dose rate of 0.35 Gy/hr (Ibrahim et al., 2018). King (2017) commented that, because waste package designs incorporate thick walls, the effect of radiation on corrosion would be small if external γ dose rates in the repository are lower than 1 Gy/hr.

Kosec et al. (2015) investigated Cu corrosion rates in oxic environments using thin electrical resistance sensors placed in a test package containing an oxic bentonite and saline groundwater environment at room temperature for a period of 4 years. Additionally, the corrosion rate was monitored by electrochemical impedance spectroscopy (EIS) measurements on the same sensors. By the end of the exposure period, the corrosion rate was estimated to have dropped to approximately 1.0 μm/yr, which also was consistent with the examination of metallographic cross sections. The corrosion products were determined to be Cu_2O and paratacamite.

Localized corrosion also may occur during this early oxidizing period, when oxidants are present to drive Cu dissolution. Researchers have shown that localized corrosion of Cu may be limited to surface roughening or under-deposit corrosion (rather than pitting) because factors that contribute to repassivation are commonly established for Cu (King et al., 1995). Of the corrosion allowance estimate of 1.27 mm over a million years during oxic and anoxic periods developed by the Canadian nuclear waste management disposal program, 0.1 mm was estimated to be a result of under-deposit corrosion, 0.17 mm from uniform corrosion, and 1 mm from microbially influenced corrosion (MIC) (Scully and Edwards, 2013).

King and Watson (2010) measured the dependence of Cu corrosion rates in compacted clay on the salinity of the groundwater. In the presence of O_2, Cu undergoes general corrosion due to the anodic dissolution of Cu coupled to the reduction of a suitable oxidant, such as dissolved O_2 or Cu(II). In chloride-dominated environments in the presence of O_2, Cu dissolves as Cu(I) with the formation of dissolved $CuCl_2^-$ ions, along with precipitated Cu_2O and $CuCl_2 \cdot 3Cu(OH)_2$ (King et al., 2001). The corrosion rates increased with O_2 concentration. Over a range of O_2

concentration, from aerated down to 0.2 volume percent of O_2 in nitrogen, the corrosion rate was between 1–25 μm/yr; however, the corrosion depth could be limited by the amount of available O_2 during the short oxidizing period.

Literature information demonstrates that Cl^- plays a significant role in corrosion of Cu, especially in oxic solutions, because Cu(I) complexation forms cuprous-chloro complex ions supported by O_2 or other cathodic reactants such as Cu^{2+} (Kear et al., 2004). The possible anodic reactions in an oxic Cl^--containing solution are:

$$Cu + Cl^- \rightarrow CuCl_{ads} + e^- \quad (2\text{-}1)$$

$$CuCl_{ads} + Cl^- \rightarrow CuCl_2^- \quad (2\text{-}2)$$

These anodic reactions are generally fast and the rates are limited by the transport of dissolved Cu(I) away from the interface. Example cathodic reactions (Betova et al., 2013) in an oxic Cl^--containing solution are:

$$O_2 + 2H_2O + 4e^- \rightarrow 4OH^- \quad (2\text{-}3)$$

$$Cu^{2+} + 2Cl^- + e^- \rightarrow CuCl_2^- \quad (2\text{-}4)$$

The cathodic reactions are probably under both electron transfer and mass transport control. When exposed to oxic environments, Cu typically forms a duplex corrosion product layer, such as an underlying layer of Cu_2O covered by $CuCl_2 \cdot 3Cu(OH)_2$, or other structures, depending on the environment (Kear et al., 2004).

2.1.2 Cu pitting corrosion and stress corrosion cracking in anoxic water with HS^-

At a later period, the groundwater contacting the waste packages is expected to be depleted of O_2, but could contain HS^-, Cl^-, SO_4^{2-}, and HCO_3^- in solution. HS^- is usually produced from two sources: (i) sulfate reducing bacteria and (ii) dissolution of pyrite (FeS_2) (SKB, 2010). According to the Pourbaix diagram, HS^- enhances Cu reaction with anoxic water, forming a copper (I) sulfide (Cu_2S) film through the following reaction:

$$2Cu + HS^- + H_2O \rightarrow Cu_2S + H_2 + OH^- \quad (2\text{-}5)$$

The depth of the corrosion front resulting from the reaction of Cu with HS^- depends on the rate of supply of HS^- present in the groundwater, and on the Cu_2S film properties including chloride (Cl^-) effects. Taniguchi and Kawasaki (2008) measured Cu corrosion rates in anoxic synthetic seawater with added sodium sulfide (Na_2S) using the weight loss method. The corrosion rate increased from less than 0.6 μm/yr, to 2 to 4 μm/yr, to 10 to 15 μm/yr as sulfide (S^{2-}) concentration increased from 0.001 M to 0.005 M to 0.1 M, respectively. In the absence of S^{2-}, the average corrosion rate was estimated to be 0.088 μm/yr over a test period of nearly 800 days.

SKB (2010) considered the reaction of Cu with HS^- in a repository environment, but this reaction was concluded to be not risk significant in SKB's safety assessment on the basis of analyses assuming (i) instant HS^- reaction with Cu as soon as it reaches the waste canister surface and (ii) limited groundwater flow rates. In the SKB analyses, the corrosion depth was controlled by the rate of supply of HS^- dissolved in groundwater and was estimated to be less than 100 μm in 1 million years (assuming well-spread damage over the waste package surface). In the updated SKB analyses (SKB, 2019), the following five issues were addressed:
(i) corrosion due to reaction in oxygen-free water; (ii) pitting due to reaction with sulfide,

including the influence of the "sauna effect" on pitting; (iii) SCC due to reaction with sulfide, including the influence of the "sauna effect" on SCC; (iv) hydrogen embrittlement; and (v) the effect of radiation on pitting, SCC, and hydrogen embrittlement. Using a combination of laboratory experiments, field testing, and numerical analyses, SKB concluded that each issue is of minor consequence to merit full consideration in a performance assessment of the geologic repository system, with the exception of pitting corrosion of the Cu canister promoted by HS^-. After implementing a simplified assessment for pitting corrosion, SKB concluded this process also would result in minor consequences that do not change the conclusions of the earlier analysis. A detailed review of recent analyses and conclusions by SKB on copper corrosion is available elsewhere (Swedish Radiation Safety Authority, 2019).

Chen et al. (2017) and King et al. (2017) conducted a series of experiments exposing Cu to S^{2-} concentrations ranging from 5×10^{-5} to 1×10^{-3} mol/L and Cl^- concentrations ranging from 0 to 5 mol/L. The authors showed that the Cu_2S film formed on the surface changed from porous to compact and protective with increasing S^{2-} concentration up to 1×10^{-4} M. Increasing Cl^- concentration increased the porosity of the film. Martino et al. (2017, 2014) showed that Cu_2S film growth is controlled by transport of HS^- or Cu^+, depending on the HS^- concentration in solution. SO_4^{2-} and HCO_3^- also affect film properties and growth. However, the effects are not as significant as Cl^- effects. Chen et al. (2019) showed that pits or localized corrosion features were observed at HS^- concentrations ≥ 5×10^{-4} mol/L. Longer solution exposure and higher Cl^- concentration led to larger localized corrosion depth. At 5×10^{-4} mol/L HS^- and 0.1 mol/L Cl^-, the deepest pit was nearly 20 times deeper than the average corrosion depth after exposure for 1,691 hours.

Taniguchi and Kawasaki (2008), Taniguchi et al. (2008, 2007), and Becker and Öijerholm (2017) reported SCC of Cu under exposure to 0.01 mol/L S^{2-} and high tensile stress. However, Bhaskaran et al. (2013), Arilahti et al. (2011), Sipilä et al. (2014), and Taxén et al. (2019, 2018) were not able to reproduce SCC. It is not conclusive whether SCC of Cu under repository environments, even in the presence of HS^-, is a potential degradation mechanism.

2.1.3 Cu corrosion in anoxic pure water

After depletion of both O_2 and HS^- in buffer and backfill materials, Cu could predominantly react with water through the following reaction as the rate of supply of HS^- in groundwater is highly constrained:

$$2Cu + 2H_2O \rightarrow 2CuOH + H_2 \quad (2\text{-}6)$$

According to the Pourbaix diagram, Cu is thermodynamically stable in anoxic environments because the H^+/H_2 equilibrium potential is lower than the Cu^+/Cu and Cu^{2+}/Cu equilibrium potential (Pourbaix, 1974), except at some extreme conditions under which the equilibrium potentials change in order.

Hultquist et al. (2009) studied Cu corrosion submerged in water in two flasks stored in air for 15 years. Cu corrosion and H_2 evolution were observed from the test. Ollila (2019, 2013) repeated the experiment in an inert atmosphere, but no Cu corrosion was observed. Research by SKB (Hedin et al., 2018) showed that no H_2 evolution is associated with Cu corrosion in anoxic water and any H_2 detected from the test was due to the original hydrogen in the material before the test. Hedin et al. (2018) concluded that corrosion of Cu in pure and anoxic water will not be sustained beyond the extent predicted by established thermodynamic data. Senior et al. (2019) immersed bundles of Cu wires in anoxic water at 50 °C [122 °F] and 75 °C [167 °F]. No

H_2 evolution was detected from the test at 50 °C [122 °F], but some H_2 was detected from the test at 75 °C [167 °F]. Assuming that the H_2 evolution was associated with Cu corrosion, the corrosion rate was on the order of 1 nm/yr.

Cleveland et al. (2014) concluded that Cu undergoes corrosion in deaerated deionized water based on EIS and polarization measurements. They concluded that in the absence of H_2, Cu will corrode on the order of 0.4 μm/yr in deionized water with an O_2 concentration on the order of, or less than, 1 ppb.

Cu reaction with water producing H_2 in anoxic conditions was considered as a "what-if" scenario in SKB (2010) assuming the following reaction:

$$2Cu + H_2O \rightarrow Cu_2O + H_2 \quad (2\text{-}7)$$

The corrosion depth was estimated to be less than 120 μm over 1 million years, based on a low equilibrium H_2 partial pressure postulated to be equal to 0.001 bar, slow diffusive transport of dissolved H_2 away from the waste container, and an implicit assumption that local hydrogen gas buildup at the canister surface slows down copper corrosion rates by the displacement of water molecules.

Scully and Edwards (2013) evaluated the corrosion depth of 1.27 mm (i.e., the corrosion allowance estimate) caused by several corrosion mechanisms (0.17 mm from general corrosion, 0.1 mm from underdeposit corrosion, and 1 mm from MIC) over a million year disposal period. The authors commented that the exact equilibrium H_2 partial pressure for Cu corrosion and reactions in the presence of a high Cl^- concentration in anoxic water are uncertain.

Boman et al. (2014) performed Cu immersion tests in pure water in autoclaves along with two reference cells without Cu. Prior to the tests, the Cu was cleaned by electropolishing, H_2 reducing, pumping, and heating in an ultra-high vacuum. The measured H_2 amount was similar for all three cells. Only a monolayer of Cu_2O was produced after 6 months of exposure at 50 ˚C [122 ˚F] accompanied by a very low concentration of copper species (4–5 μg/L) in the water. Boman et al. (2014) concluded that the oxidation rate of Cu is very low in anoxic pure water.

He et al. (2018) investigated Cu open-circuit potential (OCP), corrosion rate, and hydrogen generation under anoxic conditions using a synthetic saline groundwater based on reference compositions for deep groundwaters in crystalline rocks of the Canadian Shield. The results indicate that the Cu OCP and corrosion rates in anoxic waters (less than 10 ppb of O_2) were very sensitive to the residual O_2 concentration in solution. The corrosion rates ranged from submicrometer to micrometers per year with increasing residual O_2 concentration levels in parts per billion. Corrosion products were predominantly Cu_2O. Chlorine was present in corrosion products for tests exposed to synthetic saline groundwater. H_2 also was found to be evolved from the tests, albeit in very small amounts. However, this small amount of H_2 evolved could not be simply correlated to the Cu corrosion process because some of it could possibly have been generated from the autoclave material.

2.1.4 Cu corrosion in anoxic Cl^- solution

Cu corrosion in anoxic Cl^- solution can be expressed in the following equation:

$$2Cu\ (s) + 2H_2O\ (l) + 6Cl^-\ (aq) \rightarrow 2CuCl_3^{2-}\ (aq) + 2OH^-\ (aq) + H_2\ (g) \quad (2\text{-}8)$$

He and Ahn (2019a,b) investigated the role of Cl^- on Cu corrosion in solutions containing SO_4^{2-} and Cl^- with residual O_2 concentrations of about 0.1–0.2 ppb at 50 °C [122 °F]. SO_4^{2-} concentration was kept constant at 2×10^3 ppm, while Cl^- concentration was varied from 0 to 10^3, 10^4, and 10^5 ppm. Electrochemical methods, including corrosion potential (E_{corr}) monitoring, potentiodynamic polarization, and EIS, were used to study the Cu corrosion properties. After immersing the electrode in solution, E_{corr} reached relatively steady values in several days. E_{corr} decreased with increasing Cl^- concentration and increasing temperature. Under potentiodynamic polarization, the current increased with anodic polarization, and anodic peaks on the forward scan were observed in the solutions containing Cl^-. Beyond the peaks, there is no indication that the anodic process is suppressed by the accumulation of corrosion product deposits. During both forward and reverse scans, the potential at zero net current consistently decreased and the current density increased with increasing Cl^- concentration. Tafel slopes decreased and exchange current density also increased with increasing Cl^- concentration. The EIS data differed in solutions with different Cl^- concentrations and also differed from those obtained at 20 °C [68 °F]. Two and three time constants associated with capacitive effects, indicating a layered film structure, were determined from the EIS data. The polarization resistance derived by fitting equivalent circuits to the EIS data decreased with increasing Cl^- concentration. All these results obtained using different methods consistently demonstrated that Cl^- plays a significant role in enhancing corrosion of Cu in these solutions with extremely low O_2 concentrations. Higher temperature and higher Cl^- concentration could have depolarized the anodic reaction, resulting in lower E_{corr} values and potentially higher corrosion current (i_{corr}).

2.2 Carbon Steel Corrosion

Carbon steel is a candidate container material in a number of countries, including Belgium, Czech Republic, France, Japan, and Switzerland. Cast iron with corrosion properties similar to carbon steel is the candidate material as structural insert for the copper canister design in Sweden and Finland. The material is usually associated with repositories with clay buffer and host rocks (e.g., Opalinus clay, Boom clay, Callovo-Oxfordian clay) or with alkaline cementitious buffer. The literature information in the following sections is organized into four areas: (i) corrosion in the oxidizing period, (ii) corrosion in anoxic clay environment, (iii) corrosion in anoxic concrete porewater, and (iv) SCC.

2.2.1 Carbon steel corrosion in the oxidizing period

Dry air oxidation of carbon steel can be expressed in the following equation:

$$4Fe + 3O_2 \rightarrow 2Fe_2O_3 \quad (2\text{-}9)$$

King (2013b) summarized that the corrosion rate is a function of temperature and time in the following equation.

$$CR_{oxic} = \frac{CR_{1a}e^{-\frac{5864}{T}}}{t^{1/2}} \quad (2\text{-}10)$$

where CR_{1a} is the baseline corrosion rate, t is the time in years from the time of emplacement, and T is temperature in Kelvin (King, 2013b).

In the presence of moisture in the oxidizing period, the carbon steel corrosion reaction is

$$4Fe + 3O_2 + 2H_2O \rightarrow 4FeOOH \quad (2\text{-}11)$$

The corrosion product could change if anions such as Cl^-, SO_4^{2-}, or CO_3^{2-} are present. The reported corrosion rates vary from <1 μm/yr to 300 μm/yr, depending on the chemical composition of solution, temperature, radiation level, material properties, and test duration (King, 2013b). The corrosion rate is an Arrhenius function of temperature (King, 2013b)

$$CR_{oxic,unsaturated} = CR_{1b} e^{-\frac{1340}{T}} \quad (2\text{-}12)$$

where CR_{1b} is the baseline corrosion rate.

In a test by the Belgian nuclear waste disposal program with an unlimited supply of oxygen, the corrosion rate was measured at ~150 μm/yr in a humid clay atmosphere at 170 °C [338 °F] (Debruyn 1990) and 0.02–2 μm/yr in similar conditions but on heat-treated and welded specimens (Debruyn et al., 1991).

2.2.2 Carbon steel corrosion in anoxic clay environments

Necib et al. (2017a) determined the in-situ anaerobic corrosion rates of carbon steel materials in contact with clay and bentonite under exposure to a synthetic solution representative of Opalinus Clay porewater in a deep geological repository in Switzerland. The test period was 7 years at the Mont Terri rock laboratory. The general corrosion rate was less than 1 μm/yr determined using EIS; the corrosion product layers were composed of magnetite. The investigators also observed nonuniform general corrosion and sulfate-reducing bacterial activity. The authors commented that the corrosion rates of carbon steel in contact with clay or bentonite are expected to decrease with time because of the formation of a corrosion product layer under conditions expected in the repository.

Relevant to the Swiss disposal concept, Smart et al. (2017) also conducted corrosion experiments to determine the anaerobic corrosion rate of carbon steel in compacted bentonite under simulated deep disposal environmental conditions. The corrosion rate decreased during the experiment and reached about 0.5 μm/y after 5 years. The authors observed good agreement between carbon steel corrosion rates determined from weight loss measurements and gas generation measurements. The corrosion product was mostly magnetite. The authors also observed localized nonuniform corrosion on the surface. The Fe^{2+} released from corrosion process stained and altered the bentonite over a distance of ~150–300 μm surrounding the carbon steel specimen. Fe^{2+} was found to replace some of the Na^+ and K^+ in bentonite. Wersin et al. (2007) also observed that the dissolved ferrous species from corrosion can interact with bentonite leading to partial loss of bentonite swelling capacity by converting swelling smectite clays to nonswelling illitic forms.

Schütz et al. (2015) investigated the effect of hydrogenotrophic iron-reducing bacteria on the corrosion rate of carbon steel under simulated geological disposal conditions. In the presence of bacteria, the authors showed that the corrosion rate increased by a factor of 1.3 to 1.8. According to the authors, the bacteria enhanced corrosion by destabilizing and dissolving the passivating magnetite layer. The investigators suggested further work to address the complexity and the long-term effect of biocorrosion on materials performance for application in HLW geological disposal.

In the French HLW disposal concept, a stainless steel container placed in carbon steel overpacks will be disposed in a clay formation. Urios et al. (2014) gathered data from a 10-year in-situ experiment in which carbon steel specimens were in contact with argillite under conditions similar to those in a repository. The authors observed that iron released from carbon

steel corrosion clogged the argillite porosity at the interface and sulfur was enriched in the corrosion area, possibly as a result of the activity of sulfate reducing bacteria. Iron reducing bacteria also were found to be present at the carbon steel and argillite interface.

Martin et al. (2014) conducted a corrosion study of carbon steel embedded in anoxic saturated clay for exposure times longer than 2 years using a combination of EIS and gravimetric analysis. The authors observed a rapid corrosion rate decrease to 1 μm/yr within 2 years. The following two equations were used to describe the decreasing corrosion rates as a function of time.

$$CR\ (\mu m/yr) = 3.86t^{-0.66} \quad (2\text{-}13)$$

$$CR\ (\mu m/yr) = 4.29t^{-1} \quad (2\text{-}14)$$

where *t* is time in years.

Magnetite was found to be the main corrosion product of the inner layer. For long exposure times up to 40 months, iron sulfide and chalcopyrite were detected to be in the inner and outer layers, respectively. The authors commented that the possibility of film change over long periods of time needs to be adequately addressed and further studies are needed on the kinetics and thermodynamics of the reactions involved in forming the different layers.

Féron and Crusset (2014) gave an overview of MIC of carbon steel in the expected conditions of the French repository. In the initial oxidizing period, pyrite can be oxidized in the clay environment and sulfato-oxidant bacteria could produce sulfuric acid leading to corrosion rates of about 100–200 μm/yr. Iron reducing bacteria also may increase corrosion rates during this early period. During transient periods, localized areas with and without oxygen and with aerobic and anaerobic bacteria may be present simultaneously. These localized areas may couple to increase localized corrosion rates. Under anaerobic conditions, bacteria also may induce localized corrosion. Aside from the detrimental effect of bacteria on carbon steel, the authors showed that bacteria may have positive effects, such as consuming hydrogen and forming protective corrosion products, such as siderite. The authors commented that MIC affects materials in nuclear waste repositories, only over the short term.

Carbon steel is a candidate material for the overpack for vitrified HLW in Japan. The overpack would be surrounded by a compacted bentonite buffer in the repository at a depth of 300 m or deeper. It is expected that the buffer material surrounding the overpack will react with groundwater to produce alkaline porewater. Sakamaki et al. (2014) performed corrosion tests of carbon steel embedded in compacted bentonite in simulated groundwater. Fe_3O_4 was identified to be the corrosion product and Fe^{2+} was detected in bentonite adjacent to the carbon steel. Lee et al. (2014) investigated (i) whether iron reducing bacteria could survive in alkaline conditions in the presence of Cl^- and SO_4^{2-} and (ii) the effect of the bacteria on corrosion of the overpack. The authors showed that iron reducing bacteria can be active in these alkaline conditions with or without Cl^- and SO_4^{2-} and that the bacteria affect the corrosion process and corrosion products. Kobayashi et al. (2011) studied the corrosion behavior of a carbon steel weld joint under anaerobic conditions in contact with clay. The welded specimens were prepared using gas tungsten arc welding, gas metal arc welding, and electron beam welding. The authors reported that the general corrosion rate of carbon steel welds was lower than 10 μm/yr and that in immersion testing over 3 years the concentration of hydrogen absorbed was about 0.05 ppm. The welding process had no detrimental effect on corrosion resistance and hydrogen embrittlement.

King (2013b) showed that in anoxic conditions, carbon steel corrosion proceeds according to the following reaction:

$$Fe + 2H_2O \rightarrow Fe(OH)_2 + H_2 \quad (2\text{-}15)$$

$Fe(OH)_2$ can decompose to magnetite via the Schikkor reaction:

$$3Fe(OH)_2 \rightarrow Fe_3O_4 + 2H_2O + H_2 \quad (2\text{-}16)$$

The overall reaction for forming Fe_3O_4 and H_2 is

$$3Fe + 4H_2O \rightarrow Fe_3O_4 + 4H_2 \quad (2\text{-}17)$$

Based on literature data, King (2013b) stated that the carbon steel corrosion rate in anoxic conditions decreases with time, primarily due to the formation of surface film, and that the corrosion rate increases with temperature. In the transient anoxic period, the corrosion rate can be described with the following equation as a function of the temperature (King, 2013b)

$$CR_{anoxic,unsaturated} = CR_2 e^{-\frac{5332}{T}} \quad (2\text{-}18)$$

CR_2 is the base corrosion rate and T is the temperature in Kelvin.

Regarding the saturated anoxic period, King (2013b) noticed differences between the corrosion behavior of carbon steel in contact with aqueous solution only and in contact with compacted bentonite. In contact with compacted bentonite with carbonate, carbon steel corrodes, as in the following equation, forming carbonate-containing corrosion products.

$$Fe + CO_3^{2-} + 2H_2O \rightarrow FeCO_3 + H_2 + 2OH^- \quad (2\text{-}19)$$

General corrosion rates are usually higher in contact with clay because the formed $FeCO_3$ film is less-protective than the Fe_3O_4 film formed in contact with aqueous solution only. The corrosion rate can be described with the following equation as a function of temperature (King, 2013b)

$$CR_{anoxic,saturated} = CR_3 e^{-\frac{2435}{T}} \quad (2\text{-}20)$$

CR_3 is the base corrosion rate and T is the temperature in Kelvin.

In absence of carbonate, Fe_3O_4 is the predominant corrosion product. King (2013b) stated that the carbon steel corrosion rate in compacted clay under saturated anaerobic condition ranges from 0.1–20 μm/yr. Dillmann et al. (2014) reviewed the corrosion rates of archeological objects corroded in various media for durations exceeding 100 years. Most of the rates lie between 0.1 and 10 μm/yr.

2.2.3 Carbon steel corrosion in concrete porewater

In Belgium, the Supercontainer concept in the proposed Boom Clay repository comprises a HLW-loaded carbon steel overpack surrounded by a concrete buffer, with a stainless steel or concrete liner forming the outer boundary. The outer surface of the carbon steel overpack would be in contact with concrete porewater with pH near 12.5, expected to persist for thousands of years. The alkaline chemical environment will passivate the carbon steel. The passive film often is described as a double layer consisting of a dense inner layer and a loose outer layer. During the stable reducing period, Cl^- and sulfur species in the groundwater may penetrate the buffer and reach the carbon steel surface. A series of studies in Belgium

(Kursten et al., 2017; Kursten and Gaggiano, 2017; Smart et al., 2014) were carried out to determine the effects of radiation, temperature, Cl^-, and sulfur species on the corrosion properties of carbon steel in cementitious porewaters in an anoxic environment.

Kursten et al. (2017) and Kursten and Gaggiano (2017) conducted general corrosion, pitting corrosion, and SCC tests of carbon steel in saturated $Ca(OH)_2$ solution (pH ~12.5), saturated $Ca(OH)_2$ solution adjusted with NaOH for pH ~13.5, and artificial concrete porewater. H_2 produced from the anoxic corrosion process was measured using either a barometric gas cell or sealed autoclaves equipped with pressure transducers. Effects of temperature, gamma irradiation, Cl^- concentration, S^{2-} concentration, and $S_2O_3^{2-}$ concentration were studied over 25 and 80 °C [77 and 176 °F], 0 and 25 Gy/hr, 0 and 100 mg/L, 0 and 500 mg/L, and 0 and 100 mg/L, respectively, under anoxic conditions. Under both irradiated and nonirradiated conditions, the initially higher corrosion rates (~50 µm/yr) dropped to lower values (<0.1 µm/yr) in days. The authors showed that irradiation and the presence of Cl^-, S^{2-}, and $S_2O_3^{2-}$ did not enhance the general corrosion rate significantly. The general corrosion rates measured from H_2 generation were consistent with weight loss measurements. General corrosion rates as low as 0.03 µm/yr were obtained from tests conducted in an autoclave. The corrosion product was predominantly magnetite at 80°C [176 °F]. During potentiodynamic polarization, when the potential was swept in the positive direction, the polarization curve exhibited a wide passive range. The passive range and passivity breakdown potential decreased with increasing chloride concentration and increasing temperature, which suggests the detrimental effect of high chloride concentration and temperature on carbon steel passivity. SCC testing showed that carbon steel was not susceptible to SCC under the test conditions for base material and materials from weld and heat-affected zones and that the presence of S^{2-} up to 500 mg/L and $S_2O_3^{2-}$ did not change the SCC resistance (Kursten and Gaggiano, 2017).

He et al. (2017) investigated carbon steel passivity, corrosion rate, repassivation, hydrogen generation, and hydrogen induced cracking tendency in simulated concrete porewater under anoxic conditions, and the effects of possible anions in the porewater such as Cl^-, $S_2O_3^{2-}$, and S^{2-}. Carbon steel maintained its passivity at 50 and 80 °C [122 and 176 °F] up to a test period of 6 months and passive corrosion rates were mostly in the range of 0.1 to 0.5 µm/yr. The addition of 100 ppm Cl^-, $S_2O_3^{2-}$, and S^{2-} decreased the OCP and increased the passive dissolution current by 1.7, 1.8, and 37 times, respectively. It also led to an active carbon steel dissolution peak at approximately 0 mV_{SCE}. S^{2-} has the most detrimental and dominant effect on carbon steel passivity in concrete porewater, followed by $S_2O_3^{2-}$ and Cl^-. Under anodic polarization, carbon steel showed strong repassivation tendency in deaerated $Ca(OH)_2$ solution even in the presence of 100 ppm Cl^-, $S_2O_3^{2-}$, and S^{2-}. However, carbon steel is susceptible to crevice corrosion initiation and propagation without repassivation under open circuit conditions. H_2 evolution accompanied carbon steel passive dissolution at 80 °C [176 °F], but the material showed no hydrogen induced cracking tendency, even when the generated H_2 was contained in an autoclave and under cathodic charging over the time scale of the test.

Smart et al. (2014) studied the effects of sulfur containing species, particularly S^{2-} and $S_2O_3^{2-}$, on the anoxic corrosion rate of aerobically precorroded carbon steel. The authors reported good agreement between the gas evolution, weight loss, and electron microscopy techniques for measuring the anoxic corrosion rate of carbon steel in alkaline conditions. The presence of S^{2-} and $S_2O_3^{2-}$ in the alkaline simulant cement porewater did not cause an increase in the anoxic corrosion rate of the precorroded carbon steel.

In the current French disposal concept for medium-level radioactive waste, containers and engineered barriers will be built with reinforced concrete. Chomat et al. (2014) conducted

corrosion studies on carbon steel coupons embedded in mortar under different environmental conditions in aerated and deaerated conditions for a duration of 1 to 3 years. The average corrosion rates were <1 μm/yr. In deaerated environments, Fe_3O_4 is likely to be the corrosion product. Dissolved iron was enriched at the steel coupon and mortar interface, but it did not evolve significantly from 1 month to 3 years, indicating that corrosion rates decreased.

Waki et al. (2014) observed that the repassivation potential for crevice corrosion of carbon steel was consistently higher than the corrosion potential in a low oxygen (<0.1 volume ppm) and alkaline (pH 11.5–13.5) environment. Waki et al. (2014) conducted crevice corrosion tests under open circuit conditions for 360 days in an alkaline and anoxic environment using a combination of materials, including carbon steel, welding materials, and bolts. Crevice corrosion tests under potentiostatic conditions also were conducted for 90 days. In both tests, no localized corrosion was observed in contacts between different kinds of metals. The authors commented that crevice corrosion of carbon steel was less likely in highly alkaline and anoxic conditions.

2.2.4 Stress corrosion cracking of carbon steel

In a clay environment, carbon steel can be susceptible to SCC and hydrogen embrittlement, which has been demonstrated for oil and gas pipelines buried in clay-rich soil in the presence of carbonate. Two types of SCC have been reported (NACE International, 2013): (i) classic or intergranular, which occurs in high-pH (pH 8–11) solutions under anoxic or slightly oxic conditions and can be enhanced by hydrogen induced cracking; and (ii) transgranular, which occurs in near-neutral pH solutions under anoxic conditions. These SCC mechanisms are usually promoted by dynamic stresses, which are not expected in repository conditions. The potential effects on SCC of constant stresses, such as residual stress from fabrication or stress applied by the host rock should be evaluated.

He and Ahn (2019a) applied cathodic charging to carbon steel under static loading in simulated granitic groundwater over a temperature range of 20–80 °C [68–176 °F] to investigate hydrogen induced cracking. The test duration was up to 3 months. In one test, the solution was acidified to pH 2, and in another test the exposure surface was creviced to enhance hydrogen entry. H_2 bubbles and hydroxides were observed to form on the exposed surface under cathodic charging. However, cracking was not observed in any of the charged specimens. Similar to the high cracking resistance observed under alkaline conditions in He et al. (2017), carbon steel also showed high cracking resistance under static loading in acidified simulated granitic groundwater.

Didot et al. (2017) conducted slow strain rate and constant load tests in anoxic carbonate and bicarbonate solutions representative of water in a deep clay environment at 25 °C [77 °F] in pH 7 and 90 °C [194 °F] in pH 8 solution at potentials in the cathodic and anodic regions. The solution pH was maintained by bubbling CO_2 in equilibrium with bicarbonate under slow strain rates and also under constant load. The slow strain rate ranged from 10^{-6} to 10^{-7} s^{-1}. The authors showed that carbon steels were sensitive to environmental cracking in the testing conditions. The SCC susceptibility was enhanced for the weld metal. The authors considered hydrogen embrittlement to be responsible for the SCC susceptibility.

Necib et al. (2017b) performed calculations on stress applied by the host rock to the carbon steel casing and overpack and conducted SCC tests on carbon steel under constant load at 80 and 110 percent of the material yield strength under relevant repository environment conditions. According to Necib et al. (2017b), after a few years to a few decades, the carbon

steel material could experience tensile stress that leads to a potential risk of SCC. A crack initiation investigation showed that shallow and mostly blunted cracks formed on tensile specimens. In addition, the authors performed general corrosion tests that showed that the corrosion rate decreased from 15–25 μm/yr after exposure for 4,000 hours to 5–10 μm/yr after exposure for 8,000 hours in (i) synthetic porewater and (ii) synthetic porewater with a layer of clay deposited at the bottom of the test cell.

2.3 Titanium Corrosion

Commercially pure Ti and Ti alloys, including Ti Grades 1, 2, 5, 7, 12, and 16, have been considered as candidate waste container materials by countries such as Belgium, Canada, Czech Republic, Japan, and Sweden for repository concepts in clay or salt host rocks. The U.S. considered Ti Grades 7 and 29 for the drip shield in the proposed unsaturated Yucca Mountain repository. Because of its passivity over a wide range of environmental conditions, Ti is considered to be corrosion resistant. Pitting corrosion is usually not considered because the film breakdown potentials are several volts. The important corrosion modes for Ti are general corrosion, crevice corrosion, and hydrogen embrittlement. Compared to copper and carbon steel, Ti is a less popular candidate material for the waste container. As a result, there is limited literature information on Ti corrosion in relevant repository conditions. The following paragraphs summarize recent studies on Ti general corrosion, crevice corrosion, and hydrogen embrittlement under environmental conditions relevant to geological disposal.

Zhang et al. (2019a) conducted corrosion tests of Ti Grades 2 and 16, along with carbon steel for comparison, in simulated groundwater in contact with bentonite representative of the environment at the potential geologic repository site in the Beishan region of China. The corrosion rates of Ti Grade 2 and Grade 16 were 0.02–0.75 μm/yr and 0.02–0.15 μm/yr, respectively. Under the same environmental conditions, the carbon steel corrosion rate was much higher at 3.4–610 μm/yr. Zhang et al. (2019b) studied hydrogen entry into Ti Grade 2 in simulated repository conditions in China over the temperature range 25–100 °C [77–212 °F]. Ti hydrides formed during hydrogen charging and further diffusion of hydrogen through Ti hydrides was retarded. The compacted bentonite formed a Ca-Mg deposition layer on the Ti coupon surfaces, which also retarded hydrogen entry into Ti, but the effect was negligible compared to retardation by the Ti hydrides. Solid state hydrogen diffusivity under repository environment would be mainly affected by temperature.

Stoulil et al. (2019) investigated the susceptibility of Ti Grade 7 to hydrogen embrittlement in a synthetic bentonite porewater in the context of the Czech Republic geological repository program. The authors showed that Ti Grade 7 absorbed hydrogen in the neutral bentonite porewater at low current densities of 0.2 A/m^2. The absorbed hydrogen formed Ti hydrides in the material, leading to hydrogen embrittlement. Water radiolysis at gamma irradiation levels expected on the container surface did not lead to hydrogen absorption.

He and Ahn (2019a) conducted tests of Ti Grades 2, 7, and 29 to evaluate material passivity, crevice corrosion, and hydrogen embrittlement in a synthetic brine with composition similar to naturally occurring brines from the reservoirs in the Castile Formation near the Waste Isolation Pilot Plant site. Ti Grade 7 showed high passivity and negligible general corrosion in brines up to the highest temperature of 180 °C [356 °F] under oxic conditions. Ti Grade 7 also exhibited high crevice corrosion resistance under oxic conditions and very low hydrogen absorption efficiency under anoxic conditions, even in an acidified solution at pH 2. Ti Grade 2 showed a similar level of general corrosion resistance as Ti Grade 7 at 80 °C [176 °F], but it was susceptible to crevice corrosion. Ti Grade 29 showed lower passivity in the same

solution compared to Ti Grades 2 and 7 at 80 °C [176 °F], possibly because of its two-phase microstructure.

2.4 Stainless Steel Corrosion

Because of the passive film formed on the material surface, stainless steels are corrosion resistant materials over a wide range of environments. In oxic environments, they are susceptible to localized corrosion in the form of pitting or crevice corrosion, with Cl^- being the most common agent for initiation. Localized corrosion initiation is stochastic in nature, heavily dependent on microstructure defects as initiation sites and variable environmental conditions, and models cannot in general accurately predict long-term evolution. With the presence of stress, stainless steels also are susceptible to SCC. Because of their susceptibility to localized corrosion and SCC, stainless steels are considered as an inner container material for structural support by several countries, but not for the outer corrosion barrier for HLW and SNF disposal, for which containment is crucial and long lifetimes of at least thousands of years are required. Stainless steels are under consideration as canister materials for low- and intermediate-level waste isolation, for which absolute containment is less of a concern and long lifetimes are not required. Stainless steel canisters also are used worldwide to contain SNF during extended storage. More active research on stainless steel has been performed in the context of extended storage, with conclusions that are applicable generally to material performance in oxidizing periods. Relevant extended storage research studies are highlighted in the following sections.

2.4.1 Stainless steel pitting corrosion and stress corrosion cracking in the oxidizing period

Under atmospheric conditions, experimentally measured penetration rates for pitting and crevice corrosion are quite low. Stainless steel exposed to a saturated NaCl steam mist at 60 °C [140 °F] and 95 percent relative humidity yielded maximum penetration rates of 0.02 mm/yr [8 mils/yr] for pitting and 0.03 mm/yr for crevice corrosion (NWTRB, 2010). Davison et al. (1987) reported pitting penetration of 0.028 mm after 15 years, yielding a penetration rate of 0.0019 mm/yr. The rate of pit propagation can be much higher in aggressive environments. Morrison (1972) reported pit penetrations exceeding 0.5 mm in 304 and 316 stainless steels after a 28-month exposure at the Kennedy Space Center, Florida, yielding a penetration rate of 0.21 mm/yr. Subramanian (2007) reported that the pitting corrosion rate of Type 304 stainless steel exposed to soil at pH 5.7 can be as high as 0.9 mm/yr. A recent study by He (2019) shows that pitting corrosion can initiate at Cl^- concentration as low as 10 ppm. Once initiated, the propagation is catalytic, leading to fast penetration. At low pitting penetration rates such as 0.0019 mm/yr [0.075 mils/yr] (Davison et al., 1987), it may take thousands of years to penetrate through a 1 cm-thick container wall. However, both pitting and crevice corrosion are known to be precursors to SCC if sufficient stress exists. He et al. (2014) observed that SCC cracks consistently started at the bottom of the pits (Figure 2-1).

Most ferritic and duplex stainless steels are either immune or highly resistant to SCC; however, all austenitic grades, especially Types 304, 304L, 304LN, 316, 316L, and 316LN, have long been reported in the literature to be susceptible to chloride-induced SCC in the normal wrought condition (Grubb et al., 2005; Morgan, 1980; Kain, 1990). This susceptibility increases when the material is sensitized (He et al., 2014). In the welded condition, the heat-affected zone, which is a thin band located adjacent to the weld, can be sensitized by the precipitation of carbides, which remove chromium from the metal matrix.

(a) (b)

Figure 2-1. Examples of SCC cracks to show that pitting can be precursors to SCC (He et al., 2014)

The Electric Power Research Institute (EPRI, 2006; 2005) and the Nuclear Decommissioning Authority in the United Kingdom (Nuclear Decommissioning Authority, 2007) published review reports on SCC of stainless steel. More recently, the NRC released Information Notice (IN) 2012-20, "Potential for Chloride-Induced Stress Corrosion Cracking of Austenitic Stainless Steel and Maintenance of Dry Cask Storage Systems" (NRC, 2012). The IN describes several incidents in commercial nuclear power plants in which SCC of austenitic stainless steel components was attributed to atmospheric chloride exposure (NRC, 1999, 2010; FPL, 2005; Alexander et al., 2010). These events involved components such as emergency core cooling system piping, SNF pool cooling lines, and outdoor tanks. The IN notes that chlorides may be present in the atmosphere, not only in marine environments but also near cooling towers, salted roads, or other locations. The susceptibility of austenitic stainless steels to SCC tends to increase as the chloride concentration in the solution increases, but the level of chlorides required to produce SCC is very low and is dependent on the type of chloride salts present. The material is more resistant to SCC in NaCl solutions, but cracks readily in $MgCl_2$ solutions (Grubb et al., 2005). Increased temperature and the presence of oxygen tend to aggravate chloride-induced SCC.

In a deep repository, electrolytes from deliquescence of salt deposits on waste container surfaces could be conducive to SCC of stainless steel. SCC also requires the presence of a tensile stress, which commonly exists at welds originating from fabrication processes and contact tensions between components. Fuhr et al. (2013) stated that stresses well below yield can cause SCC and the required stress for SCC initiation decreases as the chloride concentration and temperature increase. SCC tests were performed with Type 304L C-ring specimens strained to 0.4 or 1.5 percent (He et al., 2014). At the strain of 0.4 percent, the stress on the C-ring specimen was approximately equal to the material yield stress. SCC initiation was observed on specimens deposited with 1 or 10 g/m^2 of simulated sea salt at both strain levels. Constant load tensile tests were performed on Type 304 between 0.5 and 1.75 times the material yield stress (Mayuzumi et al., 2008). Surface chloride concentration was estimated to exceed 10 g/m^2, while test conditions were 80 °C [176 °F] at 35 percent relative humidity. Specimens failed at the stress level of 0.5 times the yield stress. Additionally, the SCC initiation times are relatively short (NWTRB, 2010), with reported crack growth rates of austenitic stainless steels at the weld heat-affected zones ranging from 0.1 mm/yr (Hosler, 2010) to 0.67 mm/yr (Basson and Wicker, 2002). The significance of SCC during the oxidizing period depends on the type of stainless steel, applied and residual stresses, operating temperatures, and the presence of chlorides in the environment.

2.4.2 Stainless steel pitting corrosion and stress corrosion cracking in the reducing period

In the reducing period without O_2, localized corrosion and SCC susceptibility of stainless steels can be reduced significantly. Sridhar et al. (1995) concluded that the corrosion potential in deaerated solution was lower than the repassivation potential (Figure 2-2). As such, if the oxidizing period were very short (for example a few weeks, as estimated for the Mont Terri underground research facility in Switzerland), stainless steel may be suitable as an outer container material for HLW disposal (Necib et al., 2017a).

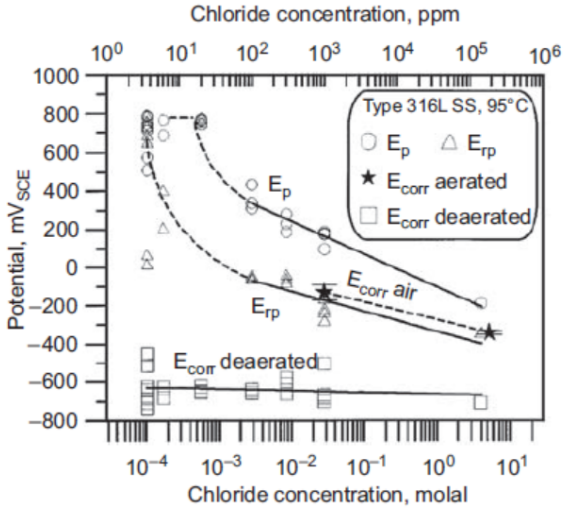

Figure 2-2. Type 316L stainless steel corrosion potential (E_{corr}) in aerated and deaearated chloride solutions, pitting potential (E_p), pit repassivation potential (E_{rp}) at 95 °C [203 °F] (Sridhar et al., 1995)

3 SUMMARY

In this chapter, inputs to the waste package corrosion model in the SOAR code and the literature information presented in Chapter 2 are summarized. Areas to be updated in SOAR are recommended.

3.1 Cu Corrosion

General corrosion is the only degradation mechanism for copper canisters considered in the current version of the NRC generic SOAR model (NRC and CNWRA, 2019). Different general corrosion rates in oxic and anoxic media, as shown in Table 3-1, were input to the model in the form of distribution functions to account for uncertainties in the rates, as well as variability in the environmental setting. Localized corrosion was not considered as a separate degradation mechanism in SOAR, but the general corrosion rates included an optional enhancement factor to account for pitting or other types of corrosion.

Table 3-1. Summary of SOAR inputs and literature information on copper corrosion

Environment	General corrosion rates (μm/yr)	Key results	References
Oxic	0.04–7 Log-uniform distribution (based on literature information before 2011)	Not applicable	SOAR User Guide (NRC and CNWRA, 2019)
	Not available	γ radiation at a total dose of 69 kGy enhances hydrogen absorption	Lousada, et al. (2016)
	Not available	In exposure to humid air, Cu_2O followed by CuO are corrosion products. Corrosion was accelerated by γ-radiation at 0.35 Gy/hr	Ibrahim et al. (2018)
	Not available	External γ dose rates are estimated to be <1 Gy/hr. Effect of radiation is expected to be small.	King (2017)
	1	Corrosion rates decreased with time. Corrosion products were Cu_2O and paratacamite.	Kosec et al. (2015)
	1–25	In Cl^--dominated oxic environment, Cu dissolves as Cu(I). Corrosion rates increased with O_2 concentration.	King and Watson (2010); King et al. (2001)
	Not available	Of the corrosion allowance estimate of 1.27 mm over a million years developed by the Canadian nuclear waste management disposal program, only 0.1 mm was estimated to be a result of surface roughening or under-deposit corrosion	Scully and Edwards (2013)

Table 3-1. Summary of SOAR inputs and literature information on copper corrosion			
Environment	**General corrosion rates (μm/yr)**	**Key results**	**References**
	Not available	Cl^- plays a significant role in Cu corrosion by complexing with Cu(I). Reaction is limited by transport of dissolved Cu(I) away from the interface. Cu typically forms a duplex corrosion product layer. Except for O_2, Cu^{2+} can also be cathodic reactant.	Kear et al. (2004); Betova et al. (2013)
Anoxic or extremely low O_2 concentration	0.004–0.02 Uniform distribution (based on literature information before year 2011)	Not applicable	SOAR User Guide (NRC and CNWRA, 2019)
	Instantaneous	HS^- is usually produced from two sources: (i) sulfate reducing bacteria and (ii) dissolution of pyrite (FeS_2). Cu corrosion limited by the rate of supply of HS^- dissolved in groundwater	SKB (2010)
	0.088–15	Corrosion rate increased as S^{2-} concentration increased from 0 to 0.1 M	Taniguchi and Kawasaki (2008)
	Not available	Cu_2S film formed on the surface changed from porous to compact and protective with increasing S^{2-} concentration up to 1×10^{-4} M. Increasing Cl^- concentration increased the porosity of the film	Chen et al. (2017); King et al. (2017)
	Not available	Cu_2S film growth is controlled by transport of HS^- or Cu^+	Martino et al. (2017, 2014)
	Not available	Pits or localized corrosion features were observed at HS^- concentrations ≥ 5×10^{-4} mol/L. Deepest pit was nearly twenty times deeper than the average corrosion depth after exposure for 1,691 hours	Chen et al. (2019)
	Not available	SCC occurred under exposure to 0.01 mol/L S^{2-} and high tensile stress	Taniguchi and Kawasaki (2008); Taniguchi et al. (2008, 2007); Becker and Öijerholm (2017)

Table 3-1. Summary of SOAR inputs and literature information on copper corrosion			
Environment	**General corrosion rates (μm/yr)**	**Key results**	**References**
	Not available	SCC was not observed under exposure to 0.01 mol/L S^{2-} and high tensile stress	Bhaskaran et al. (2013), Arilahti et al. (2011), Sipilä et al. (2014), and Taxén et al. (2019, 2018)
	Not available	Cu corrosion and H_2 evolution occurred in anoxic water	Hultquist et al. (2009)
	Not available	Cu corrosion and H_2 evolution are negligible in anoxic water	Ollila (2019, 2013); Hedin et al. (2018)
	0.001	No H_2 evolution was detected at 50 °C [122 °F], but some H_2 was detected at 75 °C [167 °F]	Senior et al. (2019)
	0.4	O_2 concentration in solution ≤1 ppb	Cleveland et al. (2014)
	0.001	1.27 mm over 1 million year. Exact equilibrium H_2 partial pressure for Cu corrosion and reactions in the presence of a high Cl^- concentration in anoxic water are uncertain.	Scully and Edwards (2013)
		Copper corrosion is very low in anoxic pure water.	Boman et al. (2014)
	0.1–5	Corrosion rates in anoxic waters (less than 10 ppb of O_2) were very sensitive to the residual O_2 concentration in solution. Corrosion products were predominantly Cu_2O.	He et al. (2018)
	Not available	Cl^- plays a significant role in enhancing corrosion of copper in these solutions with extremely low O_2 concentrations.	He and Ahn (2019)

Led by Sweden and Canada, significant research has been performed over the years to determine Cu corrosion rates and hydrogen generation in anoxic pure water. The literature shows that under anoxic conditions, corrosion rates can be enhanced by HS^- and Cl^-. Researchers tend to agree that any H_2 observed from tests in anoxic water is not produced from Cu corrosion. Instead, it pre-exists as dissolved hydrogen at interstitial and trap sites in the Cu specimens or from the test cell. However, more research using sensitive and nondestructive techniques before and after the test is needed to prove that. Another way to determine the hydrogen source is carrying out the work in heavy water (D_2O) rather than H_2O. If D_2 is generated, it is likely from corrosion of Cu. It is recommended that the SOAR model be updated so that the Cu corrosion rate in anoxic conditions accounts for the effects of both sulfide and Cl^-. The current SOAR model includes a simplified model for HS^- corrosion of copper, in which HS^- is assumed to be carried by groundwater. The HS^- contacts the canister only if there are residual gaps in the buffer material that provide a direct pathway for groundwater contact with the canister (NRC and CNWRA, 2019). If the buffer material, after saturation, fully expands and seals gaps, then it is assumed in the SOAR model that the buffer would protect the copper canister against HS^--enhanced corrosion (NRC and CNWRA, 2019). This assumption is

consistent with experiments by SKB, indicating concentrations of dissolved HS^- in bentonite porewaters below detection limits (Swedish Radiation Safety Authority, 2019).

3.2 Carbon Steel Corrosion

General corrosion of carbon steel is the main corrosion mechanism considered in the current version of SOAR. Different general corrosion rates in oxic and anoxic media are input to the model in the form of distribution functions to account for uncertainties in the rates and in the environmental setting. Pitting corrosion in oxic conditions is accounted for as an enhancement factor for the general corrosion rates. Table 3-2 summarizes the general corrosion rates and additional key results from the literature, along with the general corrosion rates input to the current SOAR model.

Table 3-2. Summary of SOAR inputs and literature information on carbon steel corrosion

Environment	General corrosion rates (μm/yr)	Additional key results	References
Oxic	10–100 Uniform distribution (based on literature information before year 2011)	Not applicable	SOAR User Guide (NRC and CNWRA, 2019)
	<1–300	Strongly depending on chemical composition of solution, temperature, radiation level, material properties, and test duration; corrosion rate generally decreases with temperature and time	King (2013b)
	150	Enhanced in a humid clay atmosphere at 170 °C [338 °F]	Debruyn (1990)
	0.02–2	Heat-treated and welded	Debruyn et al. (1991)
Anoxic or extremely low O_2 concentration	Log-normal distribution with median 1 μm/yr and geometric standard deviation equal to 2.69 (based on literature information before year 2011)	The 98 percent confidence interval was assumed to range from 0.1 to 10 μm/yr	SOAR User Guide (NRC and CNWRA, 2019)
	<1	Corrosion rate decreased with time; magnetite was the main corrosion product and possibly formed a protective layer against corrosion	Necib et al. (2017a)
	0.5	Corrosion rate decreased with time; magnetite was main corrosion product; localized non-uniform corrosion on surface embedded in compacted bentonite, Fe^{2+} interaction with bentonite	Smart et al. (2017)
	Not available	Partial loss of bentonite swelling capacity because of interaction of Fe^{2+} with bentonite	Wersin et al. (2007)

Table 3-2. Summary of SOAR inputs and literature information on carbon steel corrosion			
Environment	**General corrosion rates (μm/yr)**	**Additional key results**	**References**
	Not available	Bacteria increased corrosion rate by a factor of 1.3 to 1.8	Schütz et al. (2015)
	Not available	Corrosion product clogged argillite porosity at the interface and sulfur enriched from sulfate reducing bacteria	Urios et al. (2014)
	1	Corrosion product layer composition and structure changed over time	Martin et al. (2014)
	100–200	Bacteria can enhance localized corrosion, but bacteria also have beneficial effects	Féron and Crusset (2014)
	Not available	Magnetite as corrosion product and Fe^{2+} detected in adjacent bentonite	Sakamaki et al. (2014)
	Not available	Iron reducing bacteria could survive in alkaline conditions in the presence of Cl^- and SO_4^{2-}	Lee et al. (2014)
	<10	The welding process had no detrimental effect on corrosion resistance and hydrogen embrittlement	Kobayashi et al. (2011)
	0.1–20	Corrosion rate decreased with time primarily due to the formation of a surface film, and increased with temperature	King (2013b)
	0.1–10	Archeological objects corroded in various media for durations exceeding 100 years	Dillmann et al. (2014)
	<0.1	Detrimental effect of high chloride concentration and temperature on carbon steel passivity; base metal, heat affected zone, and weld show high resistance to SCC; negligible effect from S^{2-} and $S_2O_3^{2-}$	Kursten et al. (2017); Kursten and Gaggiano, 2017; Smart et al. (2014)
	0.1–0.5	S^{2-} has the most detrimental and dominant effect on passivity in concrete porewater, followed by $S_2O_3^{2-}$ and Cl^-; susceptible to crevice corrosion initiation and propagation; no hydrogen induced cracking observed up to 6 months test	He et al. (2017); He and Ahn (2019a)
	<1	Fe_3O_4 as main corrosion product; dissolved iron enriched at the steel coupon and mortar interface; corrosion slowed after one month	Chomat et al. (2014)
	Not available	High crevice corrosion resistance in alkaline and anoxic environment	Waki et al. (2014)
	Not available	high-pH and near-neutral pH SCC for pipeline material under dynamic load in clay environment with some carbonate	NACE International (2013)

Table 3-2. Summary of SOAR inputs and literature information on carbon steel corrosion			
Environment	**General corrosion rates (μm/yr)**	**Additional key results**	**References**
	Not available	Weld enhanced SCC susceptibility; hydrogen embrittlement responsible for SCC	Didot et al. (2017)
	5–25	Potential risk of SCC in repository environment condition	Necib et al. (2017b)

The following observations from the literature information in Table 3-2 should be considered with respect to the SOAR model for canister degradation:

- Carbon steel corrodes actively in clay environments, with corrosion rates varying depending on the properties of the clay, chemical composition of porewater, temperature, radiation level, material properties, and test duration.

- It is mostly reported that (i) corrosion rate decreases with temperature and time in both oxic and anoxic conditions, (ii) magnetite is the predominant corrosion product in anoxic conditions, (iii) the corrosion product can be protective for corrosion, (iv) corrosion products can interact with the clay and change its properties.

- In anoxic, alkaline conditions, the effects of Cl^-, S^{2-}, and $S_2O_3^{2-}$ on passivity and localized corrosion resistance are not conclusively demonstrated. The properties of the passive film and the implications of the film for localized corrosion initiation and propagation, and the enhancement factor in SOAR to account for localized corrosion, need to be evaluated further.

- Bacterial activity can enhance localized corrosion significantly. However, its effect on waste container performance over the long term is not consistently reported. The enhancement factor in SOAR to account for localized corrosion considering bacterial activity needs to be evaluated further.

- SCC and hydrogen embrittlement resistance are not consistently reported depending on types of material, thermal, environmental, and mechanical conditions, and test duration. The potential risk of SCC needs to be evaluated further for longer duration in repository environment. Its implementation in SOAR may be considered after gathering more information.

3.3 Titanium Corrosion

General corrosion of Ti is the only corrosion mechanism considered in the current version of SOAR. The same general corrosion rates for both oxic and anoxic periods are input to the model in the form of distribution functions to account for uncertainties in the rates as well as in the environmental setting. Table 3-3 summarizes the general corrosion rates and additional key results from the literature, along with the general corrosion rates in the current SOAR.

Table 3-3. Summary of SOAR inputs and literature information on titanium corrosion			
Environment	**General corrosion rates (μm/yr)**	**Additional key results**	**References**
Oxic	0.008–0.2 Log-uniform distribution (based on literature information before year 2011)	Not applicable	SOAR User Guide (NRC and CNWRA, 2019)
	Not available	Ti Grade 7 showed high passivity and negligible general corrosion in brines representative of salt rock up to the highest test temperature of 180 °C [356 °F]. Ti Grade 7 exhibited higher crevice corrosion resistance than Ti Grade 2.	He and Ahn (2019a)
Anoxic or extremely low O_2 concentration	0.008–0.2 Log-uniform distribution (based on literature information before year 2011)	Not applicable	SOAR User Guide (NRC and CNWRA, 2019)
	0.02–0.75	Titanium hydrides formed during hydrogen charging and retarded further hydrogen entry. Hydrogen diffusivity affected by temperature	Zhang et al. (2019a,b)
	Not available	Ti Grade 7 absorbed hydrogen in the neutral bentonite porewater at low current densities of 0.2 A/m^2. The absorbed hydrogen formed titanium hydrides in the material leading to hydrogen embrittlement. Water radiolysis at gamma irradiation level expected on the container surface did not lead to hydrogen absorption.	Stoulil et al. (2019)
	Not available	Ti Grade 7 had very low hydrogen absorption efficiency even at pH 2	He and Ahn (2019a)

The corrosion performance, including hydrogen absorption efficiency, of different grades of Ti can vary significantly; for example, Ti Grade 2 can absorb more hydrogen than Ti Grade 7. Therefore, under some environmental conditions hydrogen embrittlement may be a concern for Ti Grade 2, but not for Ti Grade 7. In addition to general corrosion, hydrogen embrittlement can

be an important degradation mode for some Ti grades and should be considered for incorporation in the SOAR model to account for different susceptibilities.

3.4 Stainless Steel Corrosion

General corrosion and localized corrosion of stainless steel are the main corrosion mechanisms considered in the current version of SOAR. Different general corrosion rates and fractions of stainless steel waste packages failed by localized corrosion in oxic and anoxic media are input to the model in the form of distribution functions to account for uncertainties in the rates and in the environmental setting. Table 3-4 summarizes some key results from the literature along with inputs to the current SOAR model.

Table 3-4. Summary of SOAR inputs and literature information on stainless steel corrosion

Environment	General corrosion rates (μm/yr)	Fraction of waste packages failed by localized corrosion	Key results	References
Oxic	0.01–3 Log-uniform distribution	0, 0.125, 0.25 Triangular distribution	Not applicable	SOAR User Guide (NRC and CNWRA, 2019)
	(based on literature information before year 2011)			
	Not available		Pitting corrosion rates can vary over a wide range 0.001–0.9 mm/yr depending on the type of stainless steel, environment, and test duration	NWTRB (2010), Davison et al. (1987), Morrison (1972), Subramanian (2007)
	Not available		Pitting corrosion can initiate at Cl^- concentration as low as 10 ppm. Once initiated, the propagation is catalytic leading to fast penetration	He (2019)
	Not available		Pitting corrosion is precursor to SCC	He et al. (2014)
	Not available		Stainless steel is susceptible to chloride-induced SCC. Susceptibility increases when the material is sensitized and the chloride concentration in the solution increases. The level of chlorides required to produce SCC is very low and is dependent on the type of chloride salts. SCC requires the presence of a tensile stress, which commonly exists at	Grubb et al., 2005; Morgan, 1980; Kain, 1990; He et al. (2014); EPRI (2006, 2005); Nuclear Decommissioning Authority (2007); NRC (2012, 2010, 1999); FPL (2005); Alexander et al. (2010); Grubb et al. (2005); Fuhr et al. (2013); Mayuzumi et al. (2008); NWTRB (2010);

Table 3-4. Summary of SOAR inputs and literature information on stainless steel corrosion				
Environment	**General corrosion rates (μm/yr)**	**Fraction of waste packages failed by localized corrosion**	**Key results**	**References**
			welds originating from fabrication processes and contacts between components; SCC initiation times are relatively short. Reported crack growth rates at the weld heat-affected zones ranging from 0.1 mm/yr to 0.67 mm/yr	Hosler (2010); Basson and Wicker (2002)
Anoxic or extremely low O_2 concentration	0.003–0.1 Log-uniform distribution	0.01, 0.1 Uniform distribution	Not applicable	SOAR User Guide (NRC and CNWRA, 2019)
	(based on literature information before year 2011)			
	Not available		Localized corrosion and SCC susceptibility can be reduced significantly. Corrosion potential in deaerated solution was lower than the repassivation potential	Sridhar et al. (1995)

Based on the literature information, SCC is another degradation mechanism that should be considered in the SOAR canister degradation model, especially during the oxic period, to account for potential radionuclide releases from stainless steel waste package failure.

4 REFERENCES

Alexander, D., P. Doubell, and C. Wicker. "Degradation of Safety Injection Systems and Containment Spray Piping and Tank—Fracture Toughness Analysis." Presentation at Fontevraud 7, *Contribution of Materials Investigations to Improve the Safety and Performance of LWRs*, September 26–30, 2010. Avignon, France. 2010.

Arilahti, E., T. Lehtikuusi, M. Olin, T. Saario, and P. Varis. "Evidence for Internal Diffusion of Sulphide From Groundwater Into Grain Boundaries Ahead of Crack Tip in Cu OFP Copper." *Corrosion Engineering, Science, and Technology*. Vol. 46. pp. 134–137. 2011.

Basson, J.P. and C. Wicker. "Environmentally Induced Transgranular Stress Corrosion Cracking of 304L Stainless Steel Components at Koeberg." Fontevraud 5 International Symposium, Contributions of Materials Investigations to Resolution of Problems Encountered in Pressurized Water Reactors. Société Française d'Energie Nucléaire–SFEN. Paris, France. Vol. 1–2. 1,175p. September 2002.

Becker, R. and J. Öijerholm. "Slow Strain Rate Testing of Copper in Sulfide Rich Chloride Containing Deoxygenated Water at 90 °C." Stockholm: Swedish Radiation Safety Authority. 2017.

Betova, I., M. Bojinov, and C. Lilja. "Long-Term Interaction of Copper with a Deoxygenated Neutral Aqueous Solution." *Journal of the Electrochemical Society.* Vol. 160. pp. C49–C58. 2013.

Bhaskaran G., A. Carcea, J. Ulaganathan, S. Wang, Y. Huang, and R.C. Newman. "Fundamental Aspects of Stress Corrosion Cracking of Copper relevant to the Swedish Deep Geologic Repository Concept." SKB TR-12-06. Svensk Kärnbränslehantering AB. 2013.

Boman, M., R. Berger, Y. Andersson, M. Hahlin, F. Björefors, T. Gustafsson, and M. Ottosson. "Corrosion of Copper in Water Free from Molecular Oxygen." *Corrosion Engineering, Science and Technology*. Vol. 49. pp. 431–434. 2014.

Chen J, M. Guo, T. Martino, S. Ramamurthy, J.J. Noël, D.W. Shoesmith, C. Lilja, and A.J. Johansson. "The Distribution of Corrosion Damage to Copper Surfaces Exposed to Aqueous Sulphide Solutions." SKB Document 1706406, Version 1.0, Svensk Kärnbränslehantering AB. 2019.

Chen, J., Z. Qin, T. Martino, and D.W. Shoesmith. "Effect of Chloride on Cu Corrosion in Anaerobic Sulphide Solutions." *Corrosion Engineering, Science, and Technology*. Vol. 52. pp. 40–44. 2017.

Chomat, L., V.L' Hostis, E. Amblard, and L. Bellot-Gurlet. "Long Term Study of Passive Corrosion of Steel Rebars in Portland Mortar in Context of Nuclear Waste Disposal." *Corrosion Engineering, Science and Technology.* Vol. 49. pp. 467–472. 2014.

Cleveland, C., S. Moghaddam, and M.E. Orazem. "Nanometer-Scale Corrosion of Copper in De-Aerated Deionized Water." *Journal of the Electrochemical Society*. Vol. 161. pp. C107–C114. 2014.

Davison, R.M., T. DeBold, and M.J. Johnson. "Corrosion of Stainless Steels." In ASM Handbook Vol. 13, Corrosion. Materials Park, Ohio: ASM International. pp. 547–565. 1987.

Debruyn, W. "Corrosion of Container Materials Under Clay Repository Conditions." Atomic Winnipeg, MB, Canada: Energy of Canada Limited Report AECL-10121. 1990.

Debruyn, W., J. Dresselaers, P. Vermeiren, J. Kelchtermans, and H. Tas. "Corrosion of Container and Infrastructure Materials Under Clay Repository Conditions." Commission of the European Communities Report EUR-13667. 1991.

Didot, A., E. Herms, D. Féron, J. Chêne, and D. Crusset. "Stress Corrosion Cracking in the Context of Deep Geological Nuclear Disposal–Investigations on P235 and P265 Steels." *Corrosion Engineering, Science and Technology*. Vol. 52. pp. 131–135. 2017.

Dillmann, P., D. Neff, and D. Féron. "Archaeological Analogues and Corrosion Prediction: From Past to Future. A Review." *Corrosion Engineering, Science and Technology.* Vol. 40. pp. 567–576. 2014.

EPRI. "Climatic Corrosion Considerations for Independent Spent Fuel Storage Installations in Marine Environments." Report 1013524. Palo Alto, California: Electric Power Research Institute. 2006.

_____. "Effects of Marine Environments on Stress Corrosion Cracking of Austenitic Stainless Steels." Report 1011820. Palo Alto, California: Electric Power Research Institute. 2005.

Féron, D. and D. Crusset. "Microbial Induced Corrosion in French Concept of Nuclear Waste Underground Disposal." *Corrosion Engineering, Science and Technology.* Vol. 40. pp. 540–547. 2014.

FPL. "Turkey Point Nuclear Plant Unit 3, Docket No. 50-250, 10 CFR 50.55a, Request for Temporary Non-Code Repair, Spent Fuel Pool Cooling Line." Florida Power and Light. ADAMS Accession No ML052780060. 2005.

Fuhr, K., J. Gorman, J. Broussard, and G. White. "Failure Modes and Effects Analysis (FMEA) of Welded Stainless Steel Canisters for Dry Cask Storage Systems." Palo Alto, California: Electric Power Research Institute. 2013.

Grubb, J.F., T. DeBold, and J.D. Fritz. "Corrosion of Wrought Stainless Steels." In ASM Handbook. Vol. 13B. Corrosion: Materials. Materials Park, Ohio: ASM International. pp. 54–77. 2005.

He, X. "Evaluating Pitting Corrosion of Chubu Electric Power Company Reactor Vessel Cladding." Report for Chubu Electric Power Company, Inc. 2019.

He, X. and T. Ahn. "Corrosion Studies of Carbon Steel, Copper, and Titanium as Waste Package Materials." Washington, DC: U.S. Nuclear Regulatory Commission. 2019a.

He, X. and T. Ahn. "Effects of Chloride on Copper Corrosion in Extremely Low-Oxygen Concentration Conditions." Proceedings of the CORROSION 2019 Conference. Paper No. 13134. Houston, Texas: NACE International. 2019b.

He, X. and T. Ahn. "Effects of Chloride on Copper Corrosion." Washington, DC: U.S. Nuclear Regulatory Commission. 2018.

He, X. and T. Ahn. "Effects of Chloride on Copper Corrosion and Cathodic Charging of Carbon Steel for Nuclear Waste Disposal Application." ML17304A897. Washington, DC: U.S. Nuclear Regulatory Commission. 2017a.

He, X. and T. Ahn. "Experiments on Corrosion of Copper and Carbon Steel Waste Containers—Progress Report for Fiscal Years 2015 and 2016." ML17003A453. Washington, DC: U.S. Nuclear Regulatory Commission. 2017b.

He, X., T. Ahn, and J-P. Gwo. "Corrosion of Copper as a Nuclear Waste Container Material in Simulated Anoxic Granitic Groundwater." *Corrosion.* Vol. 74. pp. 158–168. 2018.

He, X., T. Ahn, and J-P. Gwo. "Carbon Steel Corrosion in Simulated Anoxic Concrete Porewater for Nuclear Waste Disposal Application." *Corrosion*. Vol. 73. pp. 1,381–1,393. 2017.

He, X., T. Ahn, and J. McMurry. "Literature Review and Experiments on Waste Package Corrosion—Copper and Carbon Steel." ML16014A269. Washington, DC: U.S. Nuclear Regulatory Commission. 2015.

He, X., T. Mintz, R. Pabalan, L. Miller, and G. Oberson. NUREG/CR-7170, "Assessment of Stress Corrosion Cracking Susceptibility for Austenitic Stainless Steels Exposed to Chloride and Non-chloride Atmospheric Salts." 2014. http://adamswebsearch2.nrc.gov/webSearch2/main.jsp?AccessionNumber=ML14051A417

He, X., O. Pensado, T. Ahn, and P. Shukla. "Model Abstraction of Stainless Steel Waste Package Degradation." 13th International High-Level Radioactive Waste Management Conference. Albuquerque, New Mexico. 2011.

Hedin, A., A.J. Johansson, C. Lilja, M. Boman, P. Berastegui, R. Berger, and M. Ottosson. "Corrosion of Copper in Pure O_2-Free Water?" *Corrosion Science*. Vol. 137. pp. 1–12. 2018.

Hosler, R. "Screening Criteria for ID and OD-Initiated SCC of Pressure Boundary Stainless Steel Components (Phase 1 of I&E Guideline Development)." AREVA document 51-9142337-000. October 18, 2010.

Hultquist, G., P. Szakálos, M.J. Graham, G.I. Sproule, and G. Wikmark. "Detection of Hydrogen in Corrosion of Copper in Pure Water." Proceedings of the 17th International Corrosion Congress. Houston, TX: NACE International. 2009.

Ibrahim B., D. Zagidulin, M. Behazin, S. Ramamurthy, J.C. Wren, and D.W. Shoesmith. "The Corrosion of Copper in Irradiated and Unirradiated Humid Air." *Corrosion Science*. Vol.141. pp. 53–62. 2018.

Jung, H., T. Ahn, and X. He. "Representation of Copper and Carbon Steel Waste Package Degradation in a Generic Performance Assessment Model." 13th International High-Level Radioactive Waste Management Conference. Albuquerque, New Mexico. 2011.

Kain, R. “Marine Atmospheric Stress Corrosion Cracking of Austenitic Stainless Steel.” *Materials Performance*. Vol. 29, No. 12. pp. 60–62. 1990.

Kear, G., B.D. Barker, and F.C. Walsh. “Electrochemical Corrosion of Unalloyed Copper in Chloride Media—A Critical Review.” *Corrosion Science*. Vol. 46. pp. 109–135. 2004.

King, F. “Chapter 13. Nuclear waste canister materials: Corrosion behavior and long-term performance in geological repository systems.” Geological Repository Systems for Safe Disposal of Spent Nuclear Fuels and Radioactive Waste. 2nd edition. M.J. Apted and J. Ahn, eds. Elsevier Ltd. 2017.

King, F. “Container Materials for the Storage and Disposal of Nuclear Waste.” *Corrosion*. Vol. 69. pp. 986–1,011. 2013a.

King, F. “Consequences of the General Corrosion of Carbon Steel Used Fuel Containers for Gas Generation in a DGR.” NWMO TR-2013-16. Nuclear Waste Management Organization: Canada. 2013b.

King, F. and M. Kolár. “Lifetime Predictions for Nuclear Waste Disposal Containers.” *Corrosion*. Vol. 75. pp. 309–323. 2019.

King, F. and S. Watson. “Review of the Corrosion Performance of Selected Metals as Canister Materials for UK Spent Fuel and/or HLW.” QRA-1384J-1. United Kingdom: Nuclear Decommissioning Authority. 2010.

King, F., J. Chen, Z. Qin, D.W. Shoesmith, and C. Lilja. “Sulphide Mass-Transport Control of the Corrosion of Copper Canisters.” *Corrosion Engineering, Science, and Technology*. Vol. 52. pp. 210–216. 2017.

King, F., L. Ahonen, C. Taxén, U. Vuorinen, and L. Werme. “Copper Corrosion under Expected Conditions in a Deep Geologic Repository.” Technical Report TR–01–23. Svensk Kärnbränslehantering AB. Stockholm, Sweden: Swedish Nuclear Fuel and Waste Management Co. 2001.

King, F., C.D. Litke, M.J. Quinn, and D.M. LeNeveu. “The Measurement and Prediction of the Corrosion Potential of Copper in Chloride Solutions as a Function of Oxygen Concentration and Mass-Transfer Coefficient.” *Corrosion Science*. Vol. 37. pp. 833–851. 1995.

Kobayashi, M., Y. Yokoyama, R. Takahashi, H. Asano, N. Taniguchi, and M. Naito. “Long Term Integrity of Overpack Closure Weld for HLW Geological Disposal. Part 2–Corrosion Properties Under Anaerobic Conditions.” *Corrosion Engineering, Science and Technology*. Vol. 46. pp. 212–216. 2011.

Kosec, T., A. Kranjc, B. Rosborg, and A. Legat. “Post Examination of Copper ER Sensors Exposed to Bentonite.” *Journal of Nuclear Materials*. Vol. 459. pp. 306–312. 2015.

Kursten, B. and R. Gaggiano. “SCC Susceptibility of Carbon Steel Radioactive Waste Packages Exposed to Concrete Porewater Solutions Under Anoxic Conditions.” *Corrosion Engineering, Science and Technology*. Vol. 52. pp. 90–94. 2017.

Kursten, B., D.D. Macdonald, N.R. Smart, and R. Gaggiano. "Corrosion Issues of Carbon Steel Radioactive Waste Packages Exposed to Cementitious Materials With Respect to the Belgian Supercontainer Concept." *Corrosion Engineering, Science and Technology*. Vol. 52. pp. 11–16. 2017.

Lee, S., T. Matsui, and H. Yoshikawa. "Study of Microbial Corrosion Behavior of Carbon Steel Both in Alkaline Liquid Medium and Liquid Medium with Anions." *Corrosion Engineering, Science and Technology.* Vol. 40. pp. 562–566. 2014.

Lousada, C.M., I.L. Soroka, Y. Yagodzinskyy, N.V. Tarakina, O. Todoshchenko, H. Hänninen, P.A. Korzhavyi, and M. Jonsson. "Gamma Radiation Induces Hydrogen Absorption by Copper in Water." *Scientific Reports*. Vol. 6. pp. 1–8. 2016.

Martin, F., S. Perrin, M. Fenart, M. Schlegel, and C. Bataillon. "On Corrosion of Carbon Steels in Callovo-Oxfordian Clay: Complementary EIS, Gravimetric and Structural Study Providing Insights on Long Term Behavior in French Geological Disposal Conditions." *Corrosion Engineering, Science and Technology*. Vol. 49. pp. 460–466. 2014.

Martino, T., J. Chen, Z. Qin, and D.W. Shoesmith. "The Kinetics of Film Growth and Their Influence on the Susceptibility to Pitting of Copper in Aqueous Sulphide Solutions." *Corrosion Engineering, Science, and Technology*. Vol.52. pp. 61–64. 2017.

Martino, T., R. Partovi-Nia, J. Chen, Z. Qin, and D.W. Shoesmith. "Mechanisms of Film Growth on Copper in Aqueous Solutions Containing Sulphide and Chloride under Voltammetric Conditions." *Electrochimica Acta*. Vol. 127. pp. 439–447. 2014.

Mayuzumi, M., J. Tani, and T. Arai. "Chloride Induced Stress Corrosion Cracking of Candidate Canister Materials for Dry Storage of Spent Fuel." *Nuclear Engineering and Design*. Vol. 238, No. 5. pp. 1,227–1,232. 2008.

Morgan, J.D. "Report on Relative Corrosivity of Atmospheres at Various Distances from the Seacoast." NASA Report MTB 099-74. National Aeronautics and Space Administration. Cape Canaveral, Florida: Kennedy Space Center. 1980.

Morrison, J.D. "Corrosion Study of Bare and Coated Stainless Steel." NASA TN D-6519. Washington, DC: National Aeronautics and Space Administration. 1972.

NACE International. "Control of External Corrosion on Underground or Submerged Metallic Piping Systems." SP0169–2013. Houston, Texas: NACE International. 2013.

Necib, S., N. Diomidis, P. Keech, and M. Nakayama. "Corrosion of Carbon Steel in Clay Environments Relevant to Radioactive Waste Geological Disposals, Mont Terri Rock Laboratory (Switzerland)." *Swiss Journal of Geosciences*. Vol. 110. pp. 329–342. 2017a.

Necib, S., F. Bumbieler, C. Duret-Thual, N. Bulidon, D. Crusset, and P. Combrade. "Assessment of the Resistance to Environmentally Assisted Cracking (EAC) of C-steel Casing and Overpack in the COx Claystone." *Corrosion Engineering, Science and Technology*. Vol. 52. pp. 95–100. 2017b.

NRC. "Potential Chloride-Induced Stress Corrosion Cracking of Austenitic Stainless Steel and Maintenance of Dry Cask Storage System Canisters." NRC Information Notice 2012-20. Washington, DC: U.S. Nuclear Regulatory Commission. Accession No. ML12319A440. 2012.

_____. "Outside Diameter Initiated Stress Corrosion Cracking Revised Final White Paper." PA–MSC–0474." Letter (October 14) to NRC From M.L. Arey, Jr. (PWROG Owners Group). Washington, DC: U.S. Nuclear Regulatory Commission. Accession No. ML110400241. 2010

_____. "ECCS Suction Header Leaks Result in Both ECCS Trains Inoperable and TS 3.0.3 Entry." Licensee Event Report 1999-003-00. Legacy Library Accession No. 9905130085. Washington, DC: U.S. Nuclear Regulatory Commission. April 1999.

NRC and CNWRA. "SOAR: A Model for Scoping of Options and Analyzing Risk Version 2.5 User Guide." San Antonio, Texas: Center for Nuclear Waste Regulatory Analyses. April 2019.

Nuclear Decommissioning Authority. "Literature Review of Atmospheric Stress Corrosion Cracking of Stainless Steels Report to Nirex." Report No. NR3090/043. Cumbria, United Kingdom: Nuclear Decommissioning Authority. 2007.

NWTRB. "Evaluation of the Technical Basis for Extended Dry Storage and Transportation of Used Nuclear Fuel." Washington, DC: Nuclear Waste Technical Review Board. 2010.

Ollila, K. "Copper Corrosion Experiments in Pure Water Under Anoxic Conditions." Posiva Working Report 2018-19. Posiva Oy, Finland. 2019.

Ollila, K. "Copper Corrosion Experiments Under Anoxic Conditions." SKB R-13-34, Svensk Kärnbränslehantering AB. 2013.

Pourbaix, M. *Atlas of Electrochemical Equilibria in Aqueous Solutions*. 2nd Edition. Houston, Texas: NACE. 1974.

Sakamaki, K., M. Kataoka, T. Maeda, Y. Iida, M. Kamoshida, T. Yamaguchi, and T. Tanaka. "Experimental Verification of Models Assessing Eh Evolution Induced by Corrosion of Carbon Steel Overpack." *Corrosion Engineering, Science and Technology*. Vol. 49. pp. 450–454. 2014.

Schütz, M.K., M.L. Schlegel, M. Libert, and O. Bildstein. "Impact of Iron-Reducing Bacteria on the Corrosion Rate of Carbon Steel Under Simulated Geological Disposal Conditions." *Environmental Science and Technology*. Vol. 49. pp. 7,483−7,490. 2015.

Scully, J.R. and M. Edwards. "Review of the NWMO Copper Corrosion Allowance." NWMO TR-2013-04. Toronto Canada: Nuclear Waste Management Organization. May 2013.

Senior, N.A., R.C. Newman, D. Artymowicz, W.J. Binns, P.G. Keech, and D.S. Hall. "Communication—A Method to Measure Extremely Low Corrosion Rates of Copper Metal in Anoxic Aqueous Media." *Journal of the Electrochemical Society*. Vol. 166. pp. C3015–C3017. 2019.

Sipila, K., E. Arilahti, T. Lehtikuusi, and T. Saario. "Effect of Sulphide Exposure on Mechanical Properties of CuOFP." *Corrosion Engineering, Science and Technology.* Vol. 49. pp. 410–414. 2014.

SKB. “Supplementary Information on Canister Integrity Issues.” Technical Report TR-19-15. Svensk Kärnbränslehantering AB. Stockholm, Sweden: Swedish Nuclear Fuel and Waste Management Co. 2019.

_____. “Corrosion Calculations Report for the Safety Assessment SR-Site.” Technical Report TR–10–66. Svensk Kärnbränslehantering AB. Stockholm, Sweden: Swedish Nuclear Fuel and Waste Management Co. 2010.

Smart, N.R., B. Reddy, A.P. Rance, D.J. Nixon, and N. Diomidis. “The Anaerobic Corrosion of Carbon Steel in Saturated Compacted Bentonite in the Swiss Repository Concept.” *Corrosion Engineering, Science and Technology*. Vol. 52. pp. 113–126. 2017.

Smart, N.R., A.P. Rance, P.A.H. Fennell, and B. Kursten. “Effect of Sulphur Species on Anaerobic Corrosion of Carbon Steel in Alkaline Media.” *Corrosion Engineering, Science and Technology*. Vol. 49. pp. 473–479. 2014.

Sridhar, N., G.A. Cragnolino, and D.S. Dunn. “Experimental Investigations of Failure Processes of High-Level Radioactive Waste Container Materials.” CNWRA 95-010. San Antonio, Texas: Center for Nuclear Waste Regulatory Analyses. 1995.

Stoulil, J., M. Kouřil, Y.R. Carreno, D. Dobrev, J. Gondolli, and K. Nová. “Hydrogen Embrittlement of Duplex Stainless Steel 2205 and TiPd Alloy in a Synthetic Bentonite Porewater.” *Corrosion*. Vol. 75. pp. 367–376. 2019.

Subramanian, K.H. “Life Estimation of Transfer Lines for Tank Farm Closure Performance Assessment.” WSRC-STI-2007-00460. Aiken County, South Carolina: Savannah River National Laboratory. 2007.

Swedish Radiation Safety Authority. “SSM’s External Experts’ Reviews of SKB’s Report on Supplementary Information on Canister Integrity Issues.” Technical Note 2019: 22. Stockholm, Sweden: Strålsäkerhetsmyndigheten (SSM – Swedish Radiation Safety Authority). 2019.

Taniguchi, N. and M. Kawasaki. “Influence of Sulfide Concentration on the Corrosion Behavior of Pure Copper in Synthetic Seawater.” *Journal of Nuclear Materials*. Vol. 379. pp. 154–161. 2008.

Taniguchi, N., M. Kawasaki, and M. Morimasa. “Effect of Electrode Potential and Material Grade on the Behavior of Stress Corrosion Cracking of Pure Copper in Synthetic Seawater Containing Sulfide.” Japan Atomic Energy Agency Report. 2008.

Taniguchi, N., M. Kawasaki, and M. Morimasa. “Effect of Sulfide on the Corrosion Behavior of Pure Copper Under Anaerobic Condition and Possibility of Super Long Lifetime for Copper Overpacks.” JAEA-Research 2007-022. Japan Atomic Energy Agency Report. 2007.

Taxén, C., J. Flyg, and H. Bergqvist. “Stress Corrosion Testing of Copper in Near Neutral Sulfide Solutions.” SKB TR-19-13. Svensk Kärnbränslehantering AB. 2019.

Taxén, C., J. Flyg, and H. Bergqvist. “Stress Corrosion Testing of Copper in Sulfide Solutions.” SKB TR-17-16. Svensk Kärnbränslehantering AB. 2018.

Urios, L., A. Maillet, A. Dauzères, M. Flachet, and M. Magot. "Tournemire Argillite/Carbon Steel Evolution Under Bacterial Influence After 10 years of In Situ Interaction." *Corrosion Engineering, Science and Technology*. Vol. 40. pp. 554–561. 2014.

Waki, T., M. Nakagami, H. Wada, T. Ooma, O. Kato, and J. Kinugasa. "Corrosion Behavior of Waste Disposal Container in Sub-Surface Disposal System." *Corrosion Engineering, Science and Technology*. Vol. 49. pp. 503–508. 2014.

Wersin, P., L.H. Johnson, and I.G. McKinley. "Performance of the Bentonite Barrier at Temperatures Beyond 100 °C: A Critical Review." *Physics and Chemistry of the Earth*. Vol. 32. pp. 780–788. 2007.

Zhang, Q., M. Zheng, Y. Huang, H.J. Kunte, X. Wang, Y. Liu, and C. Zheng. "Long Term Corrosion Estimation of Carbon Steel, Titanium and its Alloy in Backfill Material of Compacted Bentonite for Nuclear Waste Repository." *Scientific Reports*. Vol. 9. Article No. 3195. pp. 1–18. 2019a.

Zhang, Q., Y. Huang, W. Sand, and X. Wang. "Effects of Deep Geological Environments for Nuclear Waste Disposal on the Hydrogen Entry into Titanium." *International Journal of Hydrogen Energy*. Vol. 44. pp. 12,200–12,214. 2019b.